

pubs.acs.org/est Article

# Competition of Partitioning and Reaction Controls Brown Carbon Formation from Butenedial in Particles

Jack C. Hensley,\* Adam W. Birdsall, and Frank N. Keutsch\*



Cite This: Environ. Sci. Technol. 2021, 55, 11549-11556



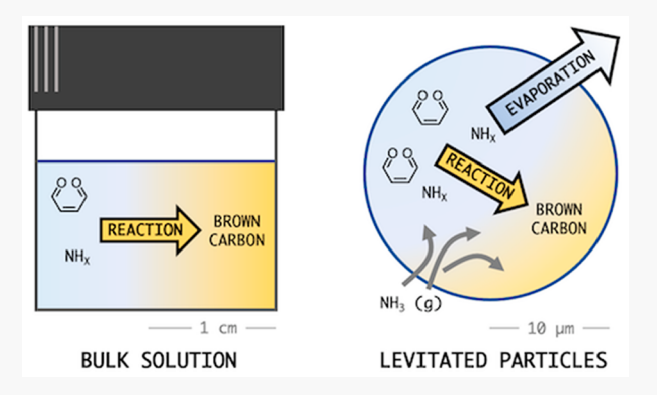
**ACCESS** I

Metrics & More

Article Recommendations

Supporting Information

ABSTRACT: Organic reactions in atmospheric particles impact human health and climate, such as by the production of brown carbon. Previous work suggests that reactions are faster in particles than in bulk solutions because of higher reactant concentrations and pronounced surface-mediated processes. Additionally, dialdehydes may have accelerated reactions in particles, as has been shown for the glyoxal reaction with ammonium sulfate (AS). Here, we examine the competition between evaporation and reaction of butenedial, a semivolatile dialdehyde, and reduced nitrogen (NH $_{\rm X}$ ) in bulk solutions and levitated particles with mass spectrometry (MS). Pyrrolinone is the major product of butenedial/AS bulk solutions, indicating brown carbon formation via accretion reactions. By contrast, pyrrolinone is completely absent in all MS measurements of comparable levitated particles suspended in a pure N $_2$  stream.



Pyrrolinone is only produced in levitated butenedial particles exposed to gas-phase ammonia, without enhanced reaction kinetics previously observed for glyoxal and other systems. Despite butenedial's large Henry's law constant and fast reaction with  $NH_X$  compared to glyoxal, the brown carbon pathway competes with evaporation only in polluted regions with extreme  $NH_X$ . Therefore, accurate knowledge of effective volatilities or Henry's law constants for complex aerosol matrices is required when chemistry studied in bulk solutions is extrapolated to atmospheric particles.

KEYWORDS: dialdehydes, brown carbon, levitated particles, aerosol mimics, surface accelerations

## 1. INTRODUCTION

Aqueous aerosol particles are important media for organic reactions in the atmosphere. No latile reactive compounds such as glyoxal and isoprene epoxydiols (IEPOX) and their reaction products are ubiquitous in atmospheric particles due to their high solubility in water. Such reactions can significantly influence particle loading and physicochemical properties, fincluding by forming low-volatility reaction products that absorb light, i.e., brown carbon. Associated implications for human health and climate depend on the speed of the reaction and its competition with other atmospheric processes.

The prevailing consensus is that reactions tend to be faster in aqueous particles than in corresponding bulk solutions. This increased rate of reaction is attributed to the high reactant concentrations of particles, which are often supersaturated compared to bulk solutions, and resulting high acidity. More recently, the surfaces of particles and other aqueous microcompartments have been thought to further accelerate reactions by influencing their energetics and kinetics. The effect of the liquid/gas interface in bulk solutions is negligible but can be important in particles, which have surface-area-to-volume (SA:V) ratios that are orders of magnitude larger than bulk solutions. Recent laboratory studies have estimated that

the surface could cause substantial (50–10<sup>6</sup> times faster<sup>7–12</sup>) accelerations on top of supersaturation effects. These findings would suggest that particle-phase chemistry can have major consequences for the composition of aerosol particles and the atmosphere. However, direct extrapolation to atmospheric particles is complicated by the high charge and short lifetimes of electrospray droplets<sup>6,8,13,14</sup> or the oil/water interface of microfluidic droplets<sup>11,15</sup> typically used in such studies. The spread in observed accelerations is one indication that we are still "scratching the surface" of chemistry in aqueous particles, including the complex ways that particle surfaces influence particle-phase reactions.

If reagents, both reactants and reaction intermediates, are sufficiently volatile, evaporation is another important process occurring at the particle surface. Evaporation can significantly reduce reaction rates when the gas phase has low reagent

Received: May 7, 2021
Revised: August 4, 2021
Accepted: August 4, 2021
Published: August 11, 2021





Table 1. List of Experiments Performed in This Study, According to Chemical System<sup>a</sup>

F	xperiment	$[BD]_0(M)$	$[NH_X]_0(M)$	[S(VI)](M)	[PEG-6] (M)	$X_{H2O}$	p <sub>NH3</sub> (ppm)
Butenedial/AS 1	oulk liquid (MS)	0.4	0.4	0.2	0.7	0.95	0
Butenedial/AS 1	particle (EDB-MS)	1.0	1.0	0.5	1.8	0.80	0
Butenedial parti	$cle + NH_3(g)$ (EDB-MS)	1.6	0	0	1.4, 1.9	0.80	0.7, 3.5, 18, 180

"Initial butenedial (BD) and reduced nitrogen (NH $_{\rm X}$ ) are provided. Other values were held constant throughout experimental runs. In the butenedial particle + NH $_{\rm 3}$  (g) experiments, PEG-6 was 1.4 M for 0.7 ppm p $_{\rm NH3}$  experimental runs and 1.9 M for 3.5, 18, and 180 ppm p $_{\rm NH3}$  experimental runs.

concentrations. For example, Daumit et al. 16 demonstrated that the OH oxidation of polyols generated volatile reaction intermediates that evaporated from submicron particles. The distribution of reaction products was shifted relative to that observed in bulk solutions, from which the evaporation of reagents is negligible. The systematic study of the influence of reactant evaporation on reaction is relevant given the recent work on surface-induced chemistry, although it is difficult with typical laboratory setups. As mentioned before, bulk solution surrogates have negligible surface effects on aqueous phase chemistry. In environmental chamber studies, populations of authentic particles live up to hours. As the gas phase often contains large concentrations of volatile reagents, the experimental setup precludes reagent evaporation from acting in isolation of condensation<sup>17</sup> and wall losses. <sup>18</sup> It is therefore difficult to isolate reagent evaporation and reaction from other processes that can occur in chambers. This is also the case in flow tubes, which additionally have experimental time scales that are much shorter than atmospheric particle lifetimes. This makes studies of the competition between gas-particle partitioning and particle chemical reactions very difficult to study when bulk reactions are slow with respect to the residence time of the flow reactor.

Alternatively, atmospheric aerosol processes can be studied in singly levitated particles. Levitated particles are capable of residing on atmospheric (hour to week) time scales in a controlled, clean gas phase. 19 Particles levitated with an electrodynamic balance tend to have only a small charge relative to electrospray droplets, <sup>20</sup> are spherical, and have radii of 10s of  $\mu m$  or greater. They are therefore relevant to deliquesced aqueous particles that are large enough to have a negligible Kelvin effect of curvature but can be supersaturated compared to bulk. Recently, the coupling of single particle levitation with an electrodynamic balance to mass spectrometry (EDB-MS) was developed by Birdsall et al. 21 and, separately, Jacobs et al.<sup>20</sup> The advantage of this technique is that chemistry can be studied at the molecular level in laboratory surrogates that replicate the shape and lifetime of atmospheric particles, enabling a faithful representation of the interaction of overlapping physicochemical processes. With EDB-MS, Birdsall et al. 21 demonstrated that vapor pressures of polyethylene glycol can be accurately estimated from multicomponent particles exposed to nitrogen gas. Jacobs et al.<sup>20</sup> estimated that a bimolecular reaction between essentially involatile reactants was 25% faster in  $\sim$ 30  $\mu$ m levitated particles compared to that in bulk solutions, a significant acceleration but one that is modest compared to those demonstrated in electrospray droplets. We build on this work by using a combination of bulk solution and levitated particle experiments to elucidate the interplay between evaporation and particle-phase reaction of volatile reactants as well as evaluate whether bulk rate constants and mechanisms apply to aerosol.

In this study, we consider whether the bimolecular reaction between butenedial, a semivolatile 1,4-dialdehyde, and reduced nitrogen (NH<sub>X</sub>, here NH<sub>X</sub> = NH<sub>3</sub> + NH<sub>4</sub><sup>+</sup>) is accelerated in particles compared to those in the bulk and how that reaction competes with evaporation. Butenedial is an atmospherically relevant product of fossil fuel combustion and biomass burning. 22-25 Research in laboratory studies has shown that oxidation of abundant volatile compounds, such as aromatics and furans, can form butenedial at molar yields comparable to those of 1,2-dicarbonyl coproducts<sup>26,27</sup> or as the dominant product.<sup>28,29</sup> We have recently characterized butenedial evaporation in salt-containing levitated particles<sup>30</sup> and reactivity in aqueous ammonia solutions. 31 The butenedial/ ammonium sulfate (AS) chemical system is similar to those in well-studied glyoxal and methylglyoxal chemistry, which is suggested to be important in the atmosphere and a source of brown carbon. 32-34 Others have found that this chemistry might be too slow to produce substantial reaction product mass under ambient conditions <sup>17,35,36</sup> compared to other loss processes, such as deposition. Some of these studies were performed in bulk solutions, and so, if surface accelerations or other particle effects are significant, this could suggest an increased role of dicarbonyl/NH<sub>X</sub> reactions in atmosphere

Like glyoxal, butenedial is hydrated extensively in aqueous media, has a large effective Henry's Law coefficient ( $6 \times 10^7$  M atm<sup>-1</sup>),<sup>30</sup> and forms brown carbon through a reaction with NH<sub>X</sub>.<sup>31</sup> In a recent study in bulk solutions, we observed a much faster butenedial/AS reaction than those of glyoxal and methylglyoxal.<sup>31</sup> Intriguingly, glyoxal/AS reactions have been shown to be accelerated in drying droplets that simulate evaporating cloud droplets.<sup>37</sup> The acceleration has in part been attributed to the preconcentration of glyoxal and AS during water removal but more substantially to the shift of dihydrated glyoxal to its reactive monohydrate, which accompanies the drying. 37-39 Additionally, glyoxal reactive uptake by AS and methylammonium salt particles was observed to increase at lower relative humidities due to enhancement of the "salting in" effect. 40,41 Butenedial reactions may not exhibit similar accelerations in drying droplets, as butenedial was not observed to preferentially form a monohydrate upon drying and is suggested to remain "kinetically frozen" as a dihydrate.<sup>3</sup> Unlike glyoxal and like methylglyoxal, butenedial vapor pressure increases ("salting out") in the presence of sulfate.<sup>30</sup> In summary, the study of the butenedial/NH<sub>X</sub> reaction and evaporation is itself atmospherically relevant and furthers our understanding of related chemical systems and their interplay in the atmosphere.

In this work, we compare the competition between the butenedial reaction with  $\mathrm{NH_X}$  and evaporation in aqueous bulk solutions and levitated particles. In the bulk solutions, evaporation is negligible, whereas in the levitated particles, reactants and products are volatilizable but are expected to be



Figure 1. Chemical structures of butenedial and major products of its reaction with  $NH_X$ . Observed mass-to-charge (m/z, of protonated compound) ratios are provided. Both cis and trans isomers are possible for BD and BD-PR.

more reactive, due to their higher concentrations and the increased SA:V. Composition is monitored with measurements of butenedial and butenedial/ $\mathrm{NH_X}$  reaction products. The previously determined Henry's law constant<sup>30</sup> and a reaction mechanism with rate constants determined from bulk studies<sup>31</sup> are used to predict the observed butenedial fate.

#### 2. METHODS

Butenedial and  $\mathrm{NH_X}$  reaction and evaporation were studied in particles levitated in an EDB and compared with previous results in bulk solutions. Experimental conditions are listed in Table 1. Measurements of the composition were taken with MS and calibrated with NMR and MS measurements of a similar reaction mixture. A custom model kinetic mechanism, combining butenedial evaporation and a previously determined butenedial/ $\mathrm{NH_X}$  reaction mechanism and rate constants, was compared against levitated particle measurements.

**2.1. Materials and Instruments.** All chemical constituents were obtained from Sigma-Aldrich unless otherwise specified. The synthesis of butenedial is described elsewhere in greater detail. Mixtures containing 2.4 M 2,5-dihydro 2,5-dimethoxyfuran (TCI America, 98%) and 3.4 M glacial acetic acid (HAc, VWR, 99.7%) were prepared. After about 10 days of reaction at room temperature, we purified mixtures with rotary evaporation to 75% butenedial by weight (w/w). The remaining 25% was predominantly residual water and HAc. All mixtures were well mixed at the start of reactions. Reacting mixtures were kept in capped glass without further stirring.

The EDB-MS apparatus is described in detail by Birdsall et al. <sup>21</sup> A droplet-on-demand particle generator injected ~140 pL aqueous particles through a charging coil into the EDB levitation chamber. A superposition of AC and DC electrodes produced an electric field that levitated particles for a defined period of time. During the levitation, 95 sccm humidified or dry nitrogen gas flowed through the EDB. Once the particle was ready to be analyzed, the gas flow and the electric field were adjusted, pushing the particle downward to impact a glass slide heated at 220 °C. The glass slide heated the particle, and a corona discharge ionized the resulting vapors to be drawn into the inlet of a commercial time-of-flight mass spectrometer (JEOL AccuTOF). The analysis was destructive: one mass spectrum could be recorded per particle. Particles were levitated for a range of residence times to track their chemical evolution.

Mass spectral signals were recorded as counts per integer mass-to-charge (m/z) channel. Hexaethylene glycol (10-20% w/w; PEG-6, 99%) was used as an internal standard for MS measurements. All other analytes are reported in counts per PEG-6 recorded at m/z 283 (the channel of the corresponding PEG-6-H<sup>+</sup> adduct), as shown in Figures S1-S3. There has

been no evidence of interactions between butenedial and PEG-6.<sup>30</sup> Distilled H<sub>2</sub>O was the solvent for all MS experiments.

2.2. Kinetic Measurements. 2.2.1. Experimental conditions and recorded species. The initial conditions in the MS kinetic experiments are reported in Table 1. Bulk solution compositions were known. Particle composition was estimated with the thermodynamic model AIOMFAC (https://aiomfac. lab.mcgill.ca/, last accessed: 2020 April 07) simulations.<sup>43</sup> These estimates reflected known relative concentrations of solutes and 75% relative humidity (RH). In the EDB experiments, RH measured with a Sensirion SHT31 probe fluctuated between 70 and 80%. The AIOMFAC calculated water mole fractions were  $0.80 \pm 0.02$  for butenedial and 0.80± 0.03 for butenedial/AS particles. The variability in water mole fraction could influence reaction and evaporation kinetics, chiefly through altering particle solute concentration, radius, and viscosity. The associated variability in calculated particle solute concentrations is 13-20%, which therefore produced variations in reaction rates and directly affected the calculated lifetimes against reaction in particles. Effects on particle viscosity were negligible. Radius and first order evaporative lifetimes were not significantly affected by the observed variability in RH. NH3 mixing ratios were calculated from the NH<sub>3</sub> bubbler concentration and assumed 75% saturation vapor pressure, as RH was 75% (see Supplemental Section 3.3 for more details). Measured species are shown in Figure 1. Butenedial (BD) was the reactant, and pyrrolinone (PR) and a butenedial-pyrrolinone "dimer" (BD-PR) were the major reaction products determined in a previous study.<sup>31</sup> For the butenedial particle +3.5 ppm of NH<sub>3</sub> experimental run, the concentrations of measured species (butenedial, pyrrolinone, and BD-PR dimer) were calculated with calibrations of the MS data (Figure S4). MS normalized signals (counts per count PEG-6) were calibrated to concentrations (molarity) with experimental data that was performed with MS and NMR.

2.2.2. Methodology. All measurements were obtained with MS by injecting particles from bulk solutions into the EDB. In the case of bulk solution measurements, particles were not trapped and simply passed through the EDB, with a purge gas of  $\sim\!250$  sccm dry nitrogen ( $N_2$ ). The particles were airborne in dry  $N_2$  for approximately 1 s during the transfer process. Water evaporation occurred at about the same time scale, causing increased reactant concentrations for a very brief period. No evidence of product formation was observed from this concentration increase.

Levitated particles were trapped in the EDB and exposed to humidified nitrogen, which was achieved by passing 95 sccm dry nitrogen through a bubbler containing distilled  $H_2O$  with or without dilute aqueous  $NH_3$  (VWR, 28-30% in  $H_2O$ ). Particle sizing measurements (typically estimated as approximately  $11-16~\mu m$  in previous work<sup>30</sup>) were not performed to

reduce transfer time, typically less than 2 min for levitated particles. The transfer time was longer for levitated particles compared to bulk solution measurements because the purge flow was increased stepwise to ~250 sccm, which ensured reliable transfer. Solution solute weight fractions were maintained at 25–30% w/w and RH at ~75% to consistently constrain particle size to similar radii. For butenedial/AS particles, reaction progress in the bulk liquid was at most 10 min before trapping, which resulted in insignificant product formation under the conditions of the bulk liquid.

Substantial shot-to-shot variability has been observed in the EDB-MS experimental setup. 21,30 Shot-to-shot variability was shown to be the major source of uncertainty in subsequent parametrizations. A previous study found no systematic sources of variability. In this study, additional variability could result from inconsistencies in transfer of reaction mixtures, flow of NH<sub>3</sub>, and composition across particles. In the quantitative comparison against model outputs, observations were clustered and the resulting error among clusters contained shot-to-shot variability and uncertainty from the calibration. The clustering was performed with Python's sklearn.cluster library using a K-means approach.

**2.3. Model Kinetic Mechanism.** The model kinetic mechanism comprised previously determined butenedial/NH<sub>X</sub> and butenedial/OH<sup>-</sup> aqueous-phase reactions<sup>31</sup> and butenedial evaporation.<sup>30</sup> The mechanism was formulated as ordinary differential equations, one ordinary differential equation per chemical compound, as shown in eqs 1–3: butenedial (BD), pyrrolinone (PR), and butenedial-pyrrolinone dimer (BD-PR). As shown in previous work, butenedial, pyrrolinone, and BD-PR dimer were reactive with accretion products (AP): oligomer-like molecules formed through the reaction. As was assumed in that study, accretion products were estimated to have the same concentration as the BD-PR dimer.<sup>31</sup>

The rate constants  $k_1-k_6$  were taken from a fit performed in a previous study.<sup>31</sup> The evaporation rate constant  $(k_e)$  was calculated from a first order fit to butenedial evaporation data reported previously in the absence of ammonium.<sup>30</sup> As is discussed in greater detail in Supporting Information Section 3.1, butenedial evaporation is approximately first order if it is sufficiently dilute, as is the case in the humid conditions and high PEG-6 content of particles in this experiment. If butenedial is the major constituent, then butenedial loss decreases particle radius and concentration, leading to a rate law that is no longer first order.  $k_e$  was found to be  $6.4 \times 10^{-3}$  $\pm$  1.5  $\times$  10<sup>-3</sup> min<sup>-1</sup> without sulfate and 6.4  $\times$  10<sup>-3</sup>  $\pm$  2.0  $\times$ 10<sup>-3</sup> min<sup>-1</sup> with 1.8 M sulfate (Figures S5, S6). A Monte Carlo simulation was performed to derive the reported 95% confidence intervals on model runs using previously reported uncertainty estimates for  $k_1$ - $k_6$  and the first order fit discussed in the Supporting Information Section 3.1 for  $k_e$ .

Particle-phase and gas-phase NH<sub>3</sub> were estimated from the known solution composition of the bubbler as described in SI Section 3.3. pH was not explicitly measured in the levitated butenedial particles. The estimated pH of 6.9 reflected the initial acidity of the particle matrix, evaporation of residual acetic acid during levitation, NH<sub>3</sub> dissolution, and the production of acid during butenedial/NH<sub>x</sub> reaction, as observed previously.<sup>31</sup> The sensitivity of model outputs to NH<sub>3</sub> and pH are shown in Figures S8 and S9, respectively, for the butenedial particle +3.5 ppm of NH<sub>3</sub> experimental run. Calculation of NH<sub>3</sub> is robust and uncertainty in NH<sub>3</sub> due to,

e.g., fluctuations in RH ( $\sim$ 5%), would not strongly affect model outputs. Over the range of pH tested (6–9), butenedial and BD-PR dimer were not found to be very sensitive to pH. Pyrrolinone was much more sensitive, although model-observation agreement of pyrrolinone was especially strong at pH 6.9. As such, although NH<sub>3</sub> and, to a greater extent, pH are unconstrained in experimental runs, they do not strongly affect overall model uncertainty, especially as it relates to butenedial reactive loss.

$$\frac{d[BD]}{dt} = -k_e[BD] - k_1[BD] - k_2[BD][NH_3] - k_3[BD][PR][OH^-] - k_4[BD][AP]$$
(1)

$$\frac{d[PR]}{dt} = k_2[BD][NH_3] - k_3[BD][PR][OH^-] - k_5[PR][AP]$$
 (2)

$$\frac{d[BD - PR]}{dt} = k_3[BD][PR][OH^-] - k_6[BD - PR][AP]$$
(3)

#### 3. RESULTS

# 3.1. Reactivity of Butenedial/AS Bulk Liquids versus Levitated Particles. In Figure 2, reaction progress is

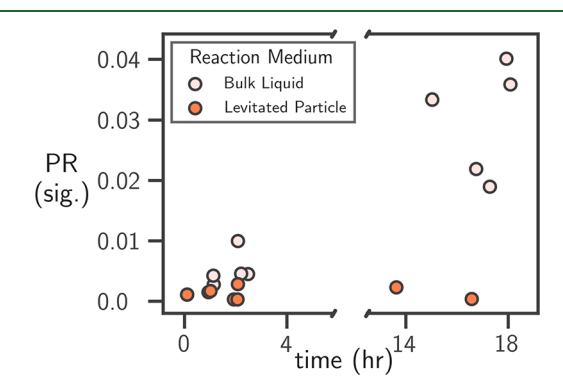


Figure 2. MS measurements of pyrrolinone (PR) are shown as a function of reaction time in butenedial/AS levitated particles and bulk liquids over 18 h, as signals normalized to PEG-6 (sig.). Levitated particles were exposed to humidified  $N_2$  gas devoid of  $NH_3$ . Pyrrolinone signal was insignificant in all measurements of levitated particles.

compared between 0.4 M butenedial/0.2 M AS bulk liquids and 1 M butenedial/0.5 M AS levitated particles without  $\mathrm{NH_3}$  in the surrounding gas phase, through MS measurements of pyrrolinone, the reaction product. Pyrrolinone accumulates in bulk liquids over several hours, but it is not detected in any recorded spectra of levitated particles over similar time scales. Reaction is expected to be accelerated in levitated particles from reactant preconcentration and from surface effects. We do not find that butenedial or pyrrolinone loss are sufficiently fast to explain the absence of pyrrolinone in levitated particles (Figure S7).  $\mathrm{NH_3}$  on the other hand has a very fast evaporation time scale on the order of seconds to minutes, 44 and competes with reaction.

**3.2.** Reactivity of Butenedial Levitated Particles Exposed to Gas Phase NH<sub>3</sub>. The dependence of butenedial/NH<sub>X</sub> reaction on NH<sub>3</sub> gas-phase mixing ratio was studied in 1.6 M butenedial levitated particles exposed to a stream of humidified N<sub>2</sub> containing NH<sub>3</sub> gas (0.7, 3.5, 18, and 180 ppm of NH<sub>3</sub>). MS measurements of butenedial and pyrrolinone at each NH<sub>3</sub> mixing ratio are shown in Figure 3.

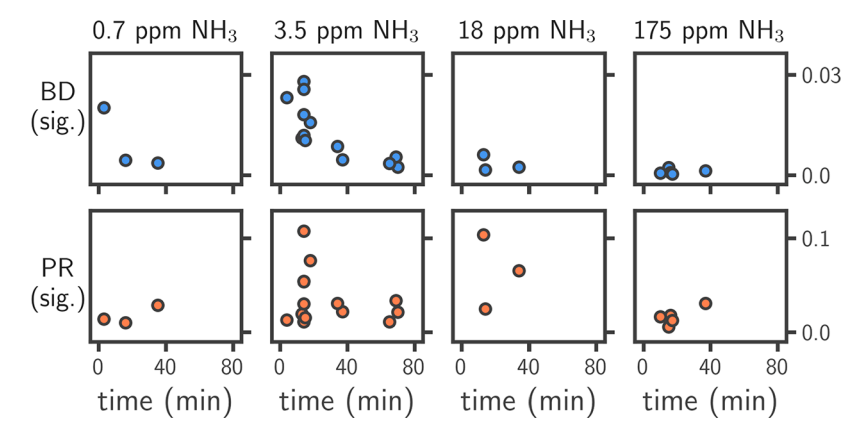


Figure 3. MS measurements of butenedial (top) and pyrrolinone (bottom) in levitated particles exposed to gas-phase NH<sub>3</sub>, shown as signals normalized to PEG-6 (sig.). Estimated gas-phase NH<sub>3</sub> are listed at the top of each column. Pyrrolinone is detected in all experimental runs, and butenedial is detected in all except at 175 ppm of NH<sub>3</sub>.

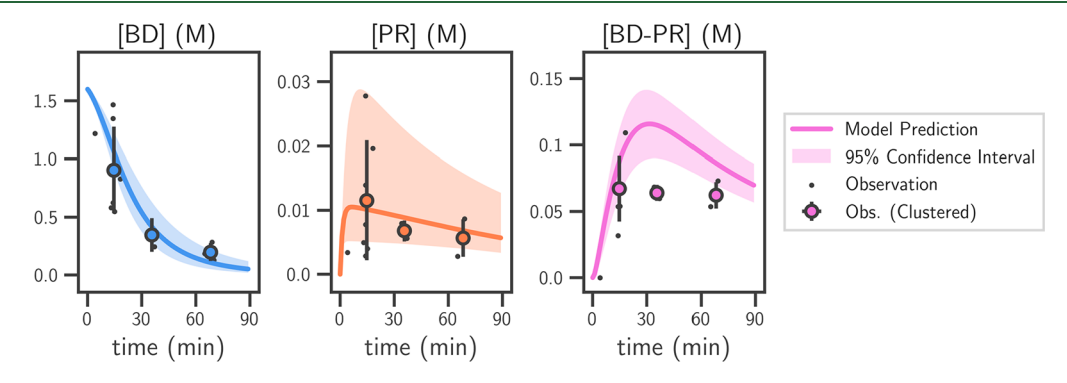
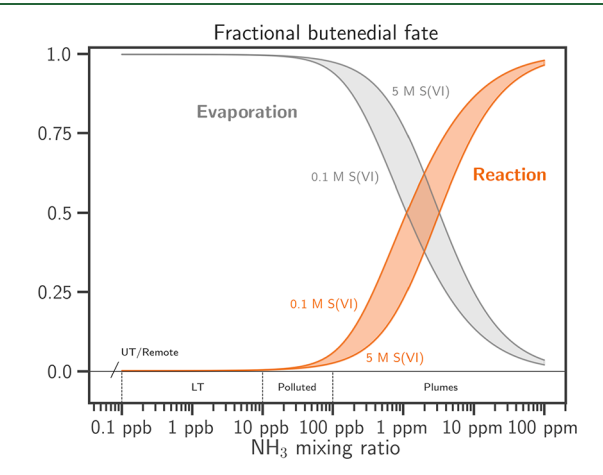


Figure 4. Comparison of measured and modeled butenedial (BD), pyrrolinone (PR), and butenedial-pyrrolinone dimer (BD-PR) concentrations in levitated butenedial particles exposed to humidified  $N_2$  gas with 3.5 ppm of  $NH_3$ . Measurements of each species are calibrated and are shown as particulate concentrations. The model is run at particle pH 6.9, 0.22 mM  $NH_3$  (the equivalent concentration of particles equilibrated with 3.5 ppm of  $NH_3$ ), and 1.6 M initial butenedial. The 95% confidence interval of model runs reflects the uncertainty in the model parametrization.

Butenedial is observed at all but the highest NH<sub>3</sub> exposure due to the fast butenedial/NH<sub>X</sub> reaction rate when exposed to 180 ppm of NH<sub>3</sub>. Pyrrolinone is detected in all measurements and is shown to be largest in the 3.5 and 18 ppm of NH<sub>3</sub> experimental runs. With high NH<sub>3</sub>, pyrrolinone formation is fast. Increased dissolution of NH<sub>3</sub> also raises the pH, which accelerates dimerization of pyrrolinone with butenedial and subsequent accretion reactions, the sinks of pyrrolinone. We suggest that pyrrolinone concentration is higher at 3.5 and 18 ppm of NH<sub>3</sub> compared to 175 ppm of NH<sub>3</sub> because the pyrrolinone loss terms are slower relative to the fast butenedial/NH<sub>X</sub> reaction.

**3.3.** Application of Model Kinetic Mechanism to Levitated Butenedial Particles Exposed to NH<sub>3</sub> Gas. The model kinetic mechanism described in eqs 1–3 was applied to the 1.6 M butenedial levitated particles exposed to 3.5 ppm of NH<sub>3</sub> gas, equivalent to 0.22 mM NH<sub>3</sub> (p). Mechanistic performance is assessed against calibrated particulate butenedial, pyrrolinone, and butenedial-pyrrolinone dimer measurements in Figure 4. The model kinetic mechanism replicates butenedial and pyrrolinone concentrations and slightly overestimates the dimer, which could be due to the calibration. We therefore do not show evidence of a significant reaction acceleration in levitated particles.

Using the model kinetic mechanism, we consider how particle pH and  $\mathrm{NH_3}$  mixing ratio modulate the competition between evaporative and reactive loss of particulate butenedial (Figure 5). The butenedial/ $\mathrm{NH_X}$  and butenedial/ $\mathrm{OH^-}$ 



**Figure 5.** Competition between evaporative and reactive loss with NH $_{\rm X}$  or OH $^-$  of butenedial is shown as a function of NH $_3$  mixing ratio and sulfur concentration, either 0.1 or 5 M. A fractional butenedial fate of 1 indicates that the loss process is totally consuming. It was assumed that butenedial concentration was 1 M and that particles were the size of those levitated in the EDB (11–16  $\mu$ m) for which the evaporation rate constant  $k_{\rm e}$  is valid. Approximate NH $_3$  mixing ratios are identified for the upper troposphere (UT)/remote, lower troposphere (LT), polluted lower troposphere, and NH $_3$  plumes.

reaction is a source of brown carbon and particle mass.<sup>31</sup> The fate of butenedial between the reactions, i.e., with OH<sup>-</sup> or

 $NH_{\rm X}$  and subsequent accretion, versus evaporation is shown as a function of  $NH_3$  mixing ratios and typical particulate sulfur concentrations, which both influence pH in atmospheric AS particles. With increased pH and  $NH_3$  mixing ratio, brown carbon reaction is a more competitive sink, which is due to pyrrolinone formation and subsequent accretion. Typical ambient  $NH_3$  mixing ratios are <10 ppb and can be 20–30 ppb in East and South Asia.  $^{45-48}$  Occasionally, 100 ppb to >1 ppm of  $NH_3$  is recorded.  $^{49-51}$  The reaction will outcompete butenedial evaporation in the atmosphere only in localized cases unless butenedial is present in the gas phase and when particulate sulfur is low.

#### 4. DISCUSSION

4.1. Surface and Bulk Processes. Not surprisingly, evaporation not only of reaction intermediates or products such as in the study of Daumit et al. 16 but also of the reactants themselves, in this case NH3, competes with reactions in the aqueous phase of particles. Presence of gas-phase NH3 allows the reaction to proceed at a rate that is competitive with the evaporation of butenedial, a semivolatile organic compound. The reaction rate in levitated particles is consistent with the model kinetic mechanism determined from bulk solutions, in spite of a  $\sim 10^3$  increase in SA:V and observed acceleration of glyoxal, another dialdehyde, reaction with NH<sub>x</sub> in evaporating droplets. Specifically, there is no evidence of acceleration of butenedial/NH<sub>X</sub> reaction by the particle surface, and it is unlikely that a significant surface effect is observed in this chemical system. The much lower charge of levitated particles compared to electrospray droplets may explain the difference in observed accelerations, in accordance with other research.<sup>13</sup> Furthermore, in contrast to glyoxal, butenedial/AS reaction is not observed to accelerate due to solvent evaporation. We suggest that because butenedial has been shown to remain "kinetically frozen" as a dihydrate at low RH, 30,31 it does not preferentially convert to its monohydrate during particle drying, a phenomenon to which Lee et al.<sup>37</sup> attribute the observed glyoxal/AS reaction rate increase. Whereas the strong "salting in" effect observed for glyoxal would enhance the competitiveness of reaction against partitioning, in the presence of sulfate, butenedial "salts out." Building off of previous work, we suggest that dialdehydes have differences in their fundamental behavior that have implications for atmospheric chemistry.

**4.2.** Atmospheric Aerosol Mimics. Bulk solutions have a long history in atmospheric research in the study of condensed phase reactions that are proposed to occur in aqueous particles. It is typically assumed that if particle concentration, pH, and ionic strength are accounted for, chemical speciation and kinetics from studies in bulk solutions are directly applicable to atmospheric particles. As enhanced reaction kinetics were not observed in levitated particles, this work suggests that the particle surface does not accelerate reactions compared to bulk solutions for the system studied here. However, bulk solutions miss the important effect of gas-particle partitioning on particle-phase chemistry. It has been shown that species like glyoxal have a speciation that depends on liquid water content,<sup>39</sup> which in atmospheric particles is predominantly modulated by relative humidity. Additionally, evaporation of volatile reaction intermediates 16 as well as reactants can reduce reaction rates. Thus, studies of bulk solutions extrapolated to atmospheric particles could overestimate the importance of chemical reactions if reactants and/or intermediates are

sufficiently volatile. We suggest that accurate knowledge of the effective volatilities or Henry's law constants for complex aerosol matrices is required when chemistry studied in bulk solutions is extrapolated to atmospheric particles.

Laboratory particles (including levitated particles, electrospray droplets, and other aqueous microcompartments) can replicate the geometry and physical and chemical properties of atmospheric aerosol particles. However, as has been suggested by others, the usage of highly charged particles may induce effects on chemistry 13 and is not relevant for atmospheric particles. The particular advantages of the levitated particles in this work, that they authentically capture the relationship between particle and surface processes on time scales relevant to the atmosphere, may not be relevant to studies where the potential chemical complexity, nonsphericity, or diffusion limitations of real particles must be considered. We propose that studies of reaction rates at lower relative humidity (where bulk diffusion could be significantly slowed), investigations of more complicated condensed phase reactions, and considerations of the role of reaction intermediate evaporation would be important steps to a further understanding of chemical reactions in aqueous aerosol particles.

4.3. Atmospheric Implications. The amount of butenedial in ambient air is largely unknown, and field observations of dicarbonyls besides methylglyoxal and glyoxal are needed to understand their effect on atmospheric chemistry. As demonstrated in Figure 5, chemical loss will rarely outcompete evaporative loss for butenedial in atmospherically relevant NH3 concentrations. However, this does not preclude the importance of this chemistry for climate. Laboratory studies have shown that even a small concentration of chromophores can significantly change the absorptive capacity of aerosol particles. 52,53 We have witnessed empirically that butenedial/ AS mixtures were darkened when less than 5% of the initial butenedial was consumed.<sup>31</sup> As such, the reaction pathway may produce brown carbon even when it is not the dominant sink of butenedial. This could, for example, be in agricultural regions that experience persistently high NH<sub>3</sub> concentrations. Brown carbon formation could be enhanced regionally if dicarbonyls and NH3 overlap. Biomass burning plumes, which can be brown in color, could contain substantial amounts of both reactants. Another atmospherically relevant scenario is where fossil fuel combustion plumes overlay agricultural or industrial plumes. This could take place, for example, in densely populated and industrial provinces in eastern China. Particle mass increases could lead to human health effects for those communities that are exposed, but they are likely outweighed by species that are coemitted in the associated combustion processes (e.g., black carbon, sulfate, other organics, nitrate).

#### ASSOCIATED CONTENT

#### Supporting Information

The Supporting Information is available free of charge at https://pubs.acs.org/doi/10.1021/acs.est.1c02891.

Experimental run information, mass spectrometry data measurement, and calibration, butenedial evaporation parametrization methods, and NH<sub>3</sub> and pH estimation and sensitivity (PDF)

#### AUTHOR INFORMATION

#### **Corresponding Authors**

Jack C. Hensley — School of Engineering and Applied Sciences, Harvard University, Cambridge, Massachusetts 02138, United States; orcid.org/0000-0002-9076-9926; Email: jhensley@g.harvard.edu

Frank N. Keutsch — School of Engineering and Applied Sciences, Department of Chemistry and Chemical Biology, and Department of Earth and Planetary Sciences, Harvard University, Cambridge, Massachusetts 02138, United States; Email: keutsch@seas.harvard.edu

#### **Author**

Adam W. Birdsall – Department of Chemistry and Chemical Biology, Harvard University, Cambridge, Massachusetts 02138, United States; Present Address: Goodyear, Akron, OH, 44316, USA

Complete contact information is available at: https://pubs.acs.org/10.1021/acs.est.1c02891

#### **Funding**

This research has been supported by the National Science Foundation, Division of Chemistry (grant no. 1808084) and the Harvard University Faculty of Arts and Sciences Dean's Competitive Fund for Promising Scholarship.

### Notes

The authors declare no competing financial interest.

#### REFERENCES

- (1) Blando, J. D.; Turpin, B. J. Secondary Organic Aerosol Formation in Cloud and Fog Droplets: A Literature Evaluation of Plausibility. *Atmos. Environ.* **2000**, *34* (10), 1623–1632.
- (2) McNeill, V. F. Aqueous Organic Chemistry in the Atmosphere: Sources and Chemical Processing of Organic Aerosols. *Environ. Sci. Technol.* **2015**, 49 (3), 1237–1244.
- (3) Pöschl, U. Atmospheric Aerosols: Composition, Transformation, Climate and Health Effects. *Angew. Chem., Int. Ed.* **2005**, 44 (46), 7520–7540
- (4) Hallquist, M.; Wenger, J. C.; Baltensperger, U.; Rudich, Y.; Simpson, D.; Claeys, M.; Dommen, J.; Donahue, N. M.; George, C.; Goldstein, A. H.; Hamilton, J. F.; Herrmann, H.; Hoffmann, T.; Iinuma, Y.; Jang, M.; Jenkin, M. E.; Jimenez, J. L.; Kiendler-Scharr, A.; Maenhaut, W.; McFiggans, G.; Mentel, T. F.; Monod, A.; Prevot, A. S. H.; Seinfeld, J. H.; Surratt, J. D.; Szmigielski, R.; Wildt, J. The Formation, Properties and Impact of Secondary Organic Aerosol: Current and Emerging Issues. *Atmos. Chem. Phys.* **2009**, *9* (14), 5155–5236.
- (5) Laskin, A.; Laskin, J.; Nizkorodov, S. A. Chemistry of Atmospheric Brown Carbon. Chem. Rev. 2015, 115 (10), 4335–4382.
- (6) Yan, X.; Bain, R. M.; Cooks, R. G. Organic Reactions in Microdroplets: Reaction Acceleration Revealed by Mass Spectrometry. *Angew. Chem., Int. Ed.* **2016**, 55 (42), 12960–12972.
- (7) Girod, M.; Moyano, E.; Campbell, D. I.; Cooks, R. G. Accelerated Bimolecular Reactions in Microdroplets Studied by Desorption Electrospray Ionization Mass Spectrometry. *Chem. Sci.* **2011**, 2 (3), 501–510.
- (8) Bain, R. M.; Pulliam, C. J.; Cooks, R. G. Accelerated Hantzsch Electrospray Synthesis with Temporal Control of Reaction Intermediates. *Chem. Sci.* **2015**, *6* (1), 397–401.
- (9) Banerjee, S.; Zare, R. N. Syntheses of Isoquinoline and Substituted Quinolines in Charged Microdroplets. *Angew. Chem.* **2015**, *127* (49), *15008*–*15012*.
- (10) Lai, Y.-H.; Sathyamoorthi, S.; Bain, R. M.; Zare, R. N. Microdroplets Accelerate Ring Opening of Epoxides. *J. Am. Soc. Mass Spectrom.* **2018**, 29 (5), 1036–1043.

- (11) Fallah-Araghi, A.; Meguellati, K.; Baret, J.-C.; Harrak, A. E.; Mangeat, T.; Karplus, M.; Ladame, S.; Marques, C. M.; Griffiths, A. D. Enhanced Chemical Synthesis at Soft Interfaces: A Universal Reaction-Adsorption Mechanism in Microcompartments. *Phys. Rev. Lett.* 2014, 112 (2), 028301.
- (12) Bain, R. M.; Pulliam, C. J.; Ayrton, S. T.; Bain, K.; Cooks, R. G. Accelerated Hydrazone Formation in Charged Microdroplets: Accelerated Reactions in Charged Microdroplets. *Rapid Commun. Mass Spectrom.* **2016**, 30 (16), 1875–1878.
- (13) Jacobs, M. I.; Davis, R. D.; Rapf, R. J.; Wilson, K. R. Studying Chemistry in Micro-Compartments by Separating Droplet Generation from Ionization. *J. Am. Soc. Mass Spectrom.* **2019**, *30* (2), 339–343.
- (14) Sahota, N.; AbuSalim, D. I.; Wang, M. L.; Brown, C. J.; Zhang, Z.; El-Baba, T. J.; Cook, S. P.; Clemmer, D. E. A Microdroplet-Accelerated Biginelli Reaction: Mechanisms and Separation of Isomers Using IMS-MS. *Chem. Sci.* **2019**, *10* (18), 4822–4827.
- (15) Song, H.; Chen, D. L.; Ismagilov, R. F. Reactions in Droplets in Microfluidic Channels. *Angew. Chem., Int. Ed.* **2006**, 45 (44), 7336–7356
- (16) Daumit, K. E.; Carrasquillo, A. J.; Hunter, J. F.; Kroll, J. H. Laboratory Studies of the Aqueous-Phase Oxidation of Polyols: Submicron Particles vs. Bulk Aqueous Solution. *Atmos. Chem. Phys.* **2014**, *14* (19), 10773–10784.
- (17) Galloway, M. M.; Chhabra, P. S.; Chan, A. W. H.; Surratt, J. D.; Flagan, R. C.; Seinfeld, J. H.; Keutsch, F. N. Glyoxal Uptake on Ammonium Sulphate Seed Aerosol: Reaction Products and Reversibility of Uptake under Dark and Irradiated Conditions. *Atmos. Chem. Phys.* **2009**, *9* (10), 3331–3345.
- (18) Zhang, X.; Cappa, C. D.; Jathar, S. H.; McVay, R. C.; Ensberg, J. J.; Kleeman, M. J.; Seinfeld, J. H. Influence of Vapor Wall Loss in Laboratory Chambers on Yields of Secondary Organic Aerosol. *Proc. Natl. Acad. Sci. U. S. A.* **2014**, *111* (16), 5802–5807.
- (19) Krieger, U. K.; Marcolli, C.; Reid, J. P. Exploring the Complexity of Aerosol Particle Properties and Processes Using Single Particle Techniques. *Chem. Soc. Rev.* **2012**, *41* (19), 6631.
- (20) Jacobs, M. I.; Davies, J. F.; Lee, L.; Davis, R. D.; Houle, F.; Wilson, K. R. Exploring Chemistry in Microcompartments Using Guided Droplet Collisions in a Branched Quadrupole Trap Coupled to a Single Droplet, Paper Spray Mass Spectrometer. *Anal. Chem.* **2017**, 89 (22), 12511–12519.
- (21) Birdsall, A. W.; Krieger, U. K.; Keutsch, F. N. Electrodynamic Balance–Mass Spectrometry of Single Particles as a New Platform for Atmospheric Chemistry Research. *Atmos. Meas. Tech.* **2018**, *11* (1), 33–47.
- (22) Coggon, M. M.; Lim, C. Y.; Koss, A. R.; Sekimoto, K.; Yuan, B.; Gilman, J. B.; Hagan, D. H.; Selimovic, V.; Zarzana, K. J.; Brown, S. S.; Roberts, J. M.; Müller, M.; Yokelson, R.; Wisthaler, A.; Krechmer, J. E.; Jimenez, J. L.; Cappa, C.; Kroll, J. H.; de Gouw, J.; Warneke, C. OH Chemistry of Non-Methane Organic Gases (NMOGs) Emitted from Laboratory and Ambient Biomass Burning Smoke: Evaluating the Influence of Furans and Oxygenated Aromatics on Ozone and Secondary NMOG Formation. *Atmos. Chem. Phys.* **2019**, *19* (23), 14875–14899.
- (23) Obermeyer, G.; Aschmann, S. M.; Atkinson, R.; Arey, J. Carbonyl Atmospheric Reaction Products of Aromatic Hydrocarbons in Ambient Air. *Atmos. Environ.* **2009**, *43* (24), 3736–3744.
- (24) Volkamer, R.; Platt, U.; Wirtz, K. Primary and Secondary Glyoxal Formation from Aromatics: Experimental Evidence for the Bicycloalkyl-Radical Pathway from Benzene, Toluene, and *p*-Xylene. *J. Phys. Chem. A* **2001**, *105* (33), 7865–7874.
- (25) Bierbach, Arwid; Barnes, Ian; Becker, K. H.; Wiesen, Evelyn Atmospheric Chemistry of Unsaturated Carbonyls: Butenedial, 4-Oxo-2-Pentenal, 3-Hexene-2,5-Dione, Maleic Anhydride, 3H-Furan-2-One, and 5-Methyl-3H-Furan-2-One. *Environ. Sci. Technol.* **1994**, 28 (4), 715–729.
- (26) Arey, J.; Obermeyer, G.; Aschmann, S. M.; Chattopadhyay, S.; Cusick, R. D.; Atkinson, R. Dicarbonyl Products of the OH Radical-Initiated Reaction of a Series of Aromatic Hydrocarbons. *Environ. Sci. Technol.* **2009**, 43 (3), 683–689.

- (27) Gómez Alvarez, E.; Viidanoja, J.; Muñoz, A.; Wirtz, K.; Hjorth, J. Experimental Confirmation of the Dicarbonyl Route in the Photo-Oxidation of Toluene and Benzene. *Environ. Sci. Technol.* **2007**, *41* (24), 8362–8369.
- (28) Gómez Alvarez, E.; Borrás, E.; Viidanoja, J.; Hjorth, J. Unsaturated Dicarbonyl Products from the OH-Initiated Photo-Oxidation of Furan, 2-Methylfuran and 3-Methylfuran. *Atmos. Environ.* **2009**, 43 (9), 1603–1612.
- (29) Aschmann, S. M.; Nishino, N.; Arey, J.; Atkinson, R. Products of the OH Radical-Initiated Reactions of Furan, 2- and 3-Methylfuran, and 2,3- and 2,5-Dimethylfuran in the Presence of NO. *J. Phys. Chem.* A 2014, 118 (2), 457–466.
- (30) Birdsall, A. W.; Hensley, J. C.; Kotowitz, P. S.; Huisman, A. J.; Keutsch, F. N. Single-Particle Experiments Measuring Humidity and Inorganic Salt Effects on Gas-Particle Partitioning of Butenedial. *Atmos. Chem. Phys.* **2019**, *19* (22), 14195–14209.
- (31) Hensley, J. C.; Birdsall, A. W.; Valtierra, G.; Cox, J. L.; Keutsch, F. N. Revisiting the Reaction of Dicarbonyls in Aerosol Proxy Solutions Containing Ammonia: The Case of Butenedial. *Atmos. Chem. Phys.* **2021**, 21 (11), 8809–8821.
- (32) Ervens, B.; Volkamer, R. Glyoxal Processing by Aerosol Multiphase Chemistry: Towards a Kinetic Modeling Framework of Secondary Organic Aerosol Formation in Aqueous Particles. *Atmos. Chem. Phys.* **2010**, *10* (17), 8219–8244.
- (33) Nozière, B.; Dziedzic, P.; Córdova, A. Formation of Secondary Light-Absorbing"""Fulvic-like""" Oligomers: A Common Process in Aqueous and Ionic Atmospheric Particles? Geophys. *Geophys. Res. Lett.* **2007**, 34 (21), L21812.
- (34) Volkamer, R.; San Martini, F.; Molina, L. T.; Salcedo, D.; Jimenez, J. L.; Molina, M. J. A Missing Sink for Gas-Phase Glyoxal in Mexico City: Formation of Secondary Organic Aerosol. *Geophys. Res. Lett.* **2007**, 34 (19), L19807.
- (35) Sedehi, N.; Takano, H.; Blasic, V. A.; Sullivan, K. A.; De Haan, D. O. Temperature- and PH-Dependent Aqueous-Phase Kinetics of the Reactions of Glyoxal and Methylglyoxal with Atmospheric Amines and Ammonium Sulfate. *Atmos. Environ.* **2013**, *77*, 656–663.
- (36) Yu, G.; Bayer, A. R.; Galloway, M. M.; Korshavn, K. J.; Fry, C. G.; Keutsch, F. N. Glyoxal in Aqueous Ammonium Sulfate Solutions: Products, Kinetics and Hydration Effects. *Environ. Sci. Technol.* **2011**, 45 (15), 6336–6342.
- (37) Lee, A. K. Y.; Zhao, R.; Li, R.; Liggio, J.; Li, S.-M.; Abbatt, Jonathan. P. D. Formation of Light Absorbing Organo-Nitrogen Species from Evaporation of Droplets Containing Glyoxal and Ammonium Sulfate. *Environ. Sci. Technol.* **2013**, 47 (22), 12819—12826.
- (38) Liggio, J. Reactive Uptake of Glyoxal by Particulate Matter. J. Geophys. Res. 2005, 110 (D10), D10304.
- (39) Loeffler, K. W.; Koehler, C. A.; Paul, N. M.; De Haan, D. O. Oligomer Formation in Evaporating Aqueous Glyoxal and Methyl Glyoxal Solutions. *Environ. Sci. Technol.* **2006**, 40 (20), 6318–6323.
- (40) Gen, M.; Huang, D. D.; Chan, C. K. Reactive Uptake of Glyoxal by Ammonium-Containing Salt Particles as a Function of Relative Humidity. *Environ. Sci. Technol.* **2018**, *52* (12), 6903–6911.
- (41) Mabato, B. R. G.; Gen, M.; Chu, Y.; Chan, C. K. Reactive Uptake of Glyoxal by Methylaminium-Containing Salts as a Function of Relative Humidity. *ACS Earth Space Chem.* **2019**, 3 (2), 150–157.
- (42) Avenati, M.; Vogel, P. Face Selectivity of TheDiels-Alder Additions of 2-Substituted 5,6-Bis((E)-Chloromethylidene)-Bicyclo[2.2.2]Octanes. *Helv. Chim. Acta* 1982, 65 (1), 204–216.
- (43) Zuend, A.; Marcolli, C.; Booth, A. M.; Lienhard, D. M.; Soonsin, V.; Krieger, U. K.; Topping, D. O.; McFiggans, G.; Peter, T.; Seinfeld, J. H. New and Extended Parameterization of the Thermodynamic Model AIOMFAC: Calculation of Activity Coefficients for Organic-Inorganic Mixtures Containing Carboxyl, Hydroxyl, Carbonyl, Ether, Ester, Alkenyl, Alkyl, and Aromatic Functional Groups. *Atmos. Chem. Phys.* 2011, 11 (17), 9155–9206.
- (44) Seinfeld, J. H.; Pandis, S. N. Atmospheric Chemistry and Physics: From Air Pollution to Climate Change; John Wiley & Sons, Incorporated: New York, 2016.

- (45) Butler, T.; Vermeylen, F.; Lehmann, C. M.; Likens, G. E.; Puchalski, M. Increasing Ammonia Concentration Trends in Large Regions of the USA Derived from the NADP/AMoN Network. *Atmos. Environ.* **2016**, *146*, 132–140.
- (46) Carmichael, G. R.; Ferm, M.; Thongboonchoo, N.; Woo, J.-H.; Chan, L. Y.; Murano, K.; Viet, P. H.; Mossberg, C.; Bala, R.; Boonjawat, J.; Upatum, P.; Mohan, M.; Adhikary, S. P.; Shrestha, A. B.; Pienaar, J. J.; Brunke, E. B.; Chen, T.; Jie, T.; Guoan, D.; Peng, L. C.; Dhiharto, S.; Harjanto, H.; Jose, A. M.; Kimani, W.; Kirouane, A.; Lacaux, J.-P.; Richard, S.; Barturen, O.; Cerda, J. C.; Athayde, A.; Tavares, T.; Cotrina, J. S.; Bilici, E. Measurements of Sulfur Dioxide, Ozone and Ammonia Concentrations in Asia, Africa, and South America Using Passive Samplers. *Atmos. Environ.* **2003**, *37* (9–10), 1293–1308.
- (47) Meng, Z. Y.; Lin, W. L.; Jiang, X. M.; Yan, P.; Wang, Y.; Zhang, Y. M.; Jia, X. F.; Yu, X. L. Characteristics of Atmospheric Ammonia over Beijing, China. *Atmos. Chem. Phys.* **2011**, *11* (12), 6139–6151.
- (48) Wang, S.; Nan, J.; Shi, C.; Fu, Q.; Gao, S.; Wang, D.; Cui, H.; Saiz-Lopez, A.; Zhou, B. Atmospheric Ammonia and Its Impacts on Regional Air Quality over the Megacity of Shanghai, China. *Sci. Rep.* **2015**, *5* (1), 15842.
- (49) Biswas, K. F.; Ghauri, B. M.; Husain, L. Gaseous and Aerosol Pollutants during Fog and Clear Episodes in South Asian Urban Atmosphere. *Atmos. Environ.* **2008**, 42 (33), 7775–7785.
- (50) Huang, C.; Chen, C. H.; Li, L.; Cheng, Z.; Wang, H. L.; Huang, H. Y.; Streets, D. G.; Wang, Y. J.; Zhang, G. F.; Chen, Y. R. Emission Inventory of Anthropogenic Air Pollutants and VOC Species in the Yangtze River Delta Region, China. *Atmos. Chem. Phys.* **2011**, *11* (9), 4105–4120.
- (51) Tevlin, A. G.; Li, Y.; Collett, J. L.; McDuffie, E. E.; Fischer, E. V.; Murphy, J. G. Tall Tower Vertical Profiles and Diurnal Trends of Ammonia in the Colorado Front Range: Tall Tower Vertical Profiles of Ammonia. *J. Geophys. Res. Atmos.* 2017, 122 (22), 12,468–12,487.
- (52) Kampf, C. J.; Jakob, R.; Hoffmann, T. Identification and Characterization of Aging Products in the Glyoxal/Ammonium Sulfate System Implications for Light-Absorbing Material in Atmospheric Aerosols. *Atmos. Chem. Phys.* **2012**, *12* (14), 6323–6333.
- (53) Shapiro, E. L.; Szprengiel, J.; Sareen, N.; Jen, C. N.; Giordano, M. R.; McNeill, V. F. Light-Absorbing Secondary Organic Material Formed by Glyoxal in Aqueous Aerosol Mimics. *Atmos. Chem. Phys.* **2009**, *9* (7), 2289–2300.